

Early Hepatic Insulin Resistance Precedes the Onset of Diabetes in Obese C57BLKS-*db/db* Mice

Richard C. Davis,¹ Lawrence W. Castellani,¹ Maryam Hosseini,^{1,2,3} Osnat Ben-Zeev,^{1,2} Hui Z. Mao,^{2,3} Michael M. Weinstein,¹ Dae Young Jung,^{4,5} John Y. Jun,⁵ Jason K. Kim,^{4,5,6} Aldons J. Lusis,¹ and Miklós Péterfy^{1,2,3}

OBJECTIVE—To identify metabolic derangements contributing to diabetes susceptibility in the leptin receptor-deficient obese C57BLKS/*J-db/db* (BKS-*db*) mouse strain.

RESEARCH DESIGN AND METHODS—Young BKS-*db* mice were used to identify metabolic pathways contributing to the development of diabetes. Using the diabetes-resistant B6-*db* strain as a comparison, in vivo and in vitro approaches were applied to identify metabolic and molecular differences between the two strains.

RESULTS—Despite higher plasma insulin levels, BKS-*db* mice exhibit lower lipogenic gene expression, rate of lipogenesis, hepatic triglyceride and glycogen content, and impaired insulin suppression of gluconeogenic genes. Hepatic insulin receptor substrate (IRS)-1 and IRS-2 expression and insulin-stimulated Akt-phosphorylation are decreased in BKS-*db* primary hepatocytes. Hyperinsulinemic-euglycemic clamp studies indicate that in contrast to hepatic insulin resistance, skeletal muscle is more insulin sensitive in BKS-*db* than in B6-*db* mice. We also demonstrate that elevated plasma triglyceride levels in BKS-*db* mice are associated with reduced triglyceride clearance due to lower lipase activities.

CONCLUSIONS—Our study demonstrates the presence of metabolic derangements in BKS-*db* before the onset of β -cell failure and identifies early hepatic insulin resistance as a component of the BKS-*db* phenotype. We propose that defects in hepatic insulin signaling contribute to the development of diabetes in the BKS-*db* mouse strain. *Diabetes* 59:1616–1625, 2010

Established in the 1940s, the C57BLKS (BKS) inbred mouse strain represents one of the first animal models of type 2 diabetes (1). Development of diabetes in these mice captures several aspects of the human disease (2,3). First, diabetes in this model is associated with obesity. Whereas lean BKS mice

are normoglycemic throughout their life, obese leptin-deficient (BKS-*ob*) or leptin receptor-deficient (BKS-*db*) mice develop severe hyperglycemia. Second, the natural history of diabetes in BKS-*ob* or BKS-*db* is reminiscent of the human disease. These mice initially compensate for obesity-associated insulin resistance by increasing plasma insulin levels, but exhibit β -cell failure and insulin deficiency later in life. Finally, similarly to humans, diabetes in BKS-*db* is determined by multiple genetic factors (4,5). Despite extensive genetic analysis, the genes responsible for diabetes susceptibility in the BKS strain remain to be identified (6–8).

Early studies on BKS-*db* mice indicated that the development of diabetes is associated with progressive β -cell degeneration and a precipitous decrease in β -cell mass and plasma insulin levels (2). In vivo radio-labeling studies revealed that after an initial phase of hyperproliferation at 4–6 weeks of age, the replication of β -cells gradually decreases despite increasing glucose levels (9). In contrast to BKS, introduction of the *db* mutation into the C57BL/6J (B6) genetic background produces a dramatically different β -cell phenotype (2,4). Although similarly obese as BKS-*db*, B6-*db* mice compensate for insulin resistance by β -cell hyperplasia, increased islet mass, and hyperinsulinemia and maintain only mildly elevated blood glucose levels throughout their life. The markedly different β -cell responses to obesity in BKS-*db* and B6-*db* mice suggest that genetically determined variation in β -cell viability/survival in the face of chronic glycemic stress is responsible for differences in diabetes susceptibility between the two strains. Consistent with this hypothesis, BKS β -cells are more sensitive than B6 to cell death triggered by β -cell toxins, such as alloxan and streptozotocin (10–12), and glucose-stimulated islet cell replication is diminished in BKS (13). In conclusion, previous studies suggest that variant β -cell functions underlie the differences in diabetes susceptibility between BKS-*db* and B6-*db* mice.

In the current study, we refine the current β -cell-centric model of diabetes susceptibility in BKS-*db* by demonstrating metabolic defects preceding the onset of β -cell failure. In particular, BKS-*db* mice exhibit elevated hepatic insulin resistance associated with altered lipogenic and gluconeogenic pathways relative to B6-*db*. We propose that early hepatic insulin resistance contributes to the development of diabetes in the BKS-*db* strain.

RESEARCH DESIGN AND METHODS

Animals. C57BL/6J-*db/db* (B6-*db*) and C57BLKS/*J-db/db* (BKS-*db*) mice were purchased from The Jackson Laboratory. Mice were maintained in the animal care facilities of the University of California and VA Greater Los Angeles Healthcare System on a 12-h light/dark cycle. The mice were maintained on a standard diet (Harlan Teklad LM-485). Before all experiments, mice were fasted for 4 h (9:00 A.M. to 1:00 P.M.) unless indicated otherwise. Protocols were

From the ¹Department of Medicine, University of California, Los Angeles, Los Angeles, California; the ²Lipid Research Laboratory, VA Greater Los Angeles Healthcare System, Los Angeles, California; the ³Medical Genetics Institute, Cedars-Sinai Medical Center, Los Angeles, California; the ⁴Program in Molecular Medicine, Division of Endocrinology, Metabolism and Diabetes, University of Massachusetts Medical School, Worcester, Massachusetts; the ⁵Department of Cellular and Molecular Physiology, Pennsylvania State University School of Medicine, Hershey, Pennsylvania; and the ⁶Department of Medicine, Division of Endocrinology, Metabolism and Diabetes, University of Massachusetts Medical School, Worcester, Massachusetts.

Corresponding author: Miklós Péterfy, mpeterfy@ucla.edu.

Received 11 June 2009 and accepted 5 April 2010. Published ahead of print at <http://diabetes.diabetesjournals.org> on 14 April 2010. DOI: 10.2337/db09-0878.

R.C.D. and L.W.C. contributed equally to this work.

© 2010 by the American Diabetes Association. Readers may use this article as long as the work is properly cited, the use is educational and not for profit, and the work is not altered. See <http://creativecommons.org/licenses/by-nc-nd/3.0/> for details.

The costs of publication of this article were defrayed in part by the payment of page charges. This article must therefore be hereby marked "advertisement" in accordance with 18 U.S.C. Section 1734 solely to indicate this fact.

approved by the Institutional Animal Care and Use Committees of the respective institutions.

Phenotypic characterization of mice. Plasma lipids, glucose, and insulin were determined as described previously (14). The Luminex 100 system was used to measure plasma leptin, resistin, tumor necrosis factor- α , and interleukin-6 levels. Adiponectin, corticosterone (R&D Systems, Minneapolis, MN), and glucagon (ALPCO Diagnostics, Salem, NH) were determined by enzyme-linked immunosorbent assays. Hepatic glycogen content was assayed at the Mouse Metabolic Phenotyping Center at Yale University. Hepatic triglyceride (TG) content was assayed using the L-type TG H kit (Wako Diagnostics, Richmond, VA) with modifications. Briefly, liver tissue was homogenized in ice-cold PBS with a Polytron homogenizer. After Folch extraction, samples were centrifuged and the lower (organic) phase was transferred to new tubes. The organic volume was dried in vacuum and re-dissolved in 90 μ l of 10% Triton X-100 in isopropanol by vortexing. After the addition of 1.5 ml Wako Reagent A, samples were vortexed and incubated at 37°C for 5 min. Samples were vortexed until clear and 0.75 ml Wako Reagent B was added followed by incubation at 37°C for 30 min. Samples were vortexed again until clear and then put on ice until measurement of optical density at 600 nm. A calibration curve was established using the Wako Lipid Calibrator.

Assays of lipid metabolism. Fatty acid (FA) synthesis and oxidation were measured in liver slice cultures (15).

FA oxidation. After an overnight fast, mice were anesthetized with isoflurane and killed by cervical dislocation. The left caudal lobe of the liver was rapidly excised, and fresh liver sections of uniform thickness (1 mm, averaging ~60 mg) were obtained using a Stadie-Riggs microtome. The liver sections were weighed and immediately incubated at 37°C for 40 min in Krebs-Henseleit buffer under 95% O₂:5% CO₂ that contained 5.5 mmol/l glucose, 3% BSA, 1 mmol/l oleate, and [¹⁴C]-palmitic acid (2.5 μ Ci/ml). The average time from euthanizing the animals to getting the liver section into the buffer was <2 min. Rates of FA oxidation were assessed by determining ¹⁴CO₂ trapped in hyamine hydroxide saturated filter paper as described previously (16).

Hepatic lipogenesis. Liver sections were obtained and incubated essentially as described above, except that ³H₂O (0.5 mCi/vessel) was used as the radioactive tracer and incubations were carried out for 1 h (17). Media and tissue were then collected and total lipids extracted as described above. Total lipid isolates were then hydrolyzed in an acid/acetonitrile solution as described previously (18), and the lipids were re-extracted and dried under nitrogen and radioactivity in the fatty acid fraction determined by liquid scintillation spectrometry.

Hepatic TG secretion. TG secretion was determined by comparing plasma TG levels at 0 and 30 min after intravenous injection of Triton WR1339 (Tyloxapol, Sigma Chemical) as described (19). Calculations assumed plasma volume of 3.5% of body weight.

Triglyceride clearance. Clearance of TG (10 μ l peanut oil/g body weight delivered by gavage) was determined by following plasma TG levels at hourly intervals after the administration of lipid.

Post-heparin plasma. Ten units of heparin was administered by tail-vein injection followed by retro-orbital blood collection 10 min later as described (20). Plasma lipase activities were determined as described below.

Gene expression. Total RNA was isolated with Trizol (Invitrogen) and reverse transcribed using the Omniscript RT kit (Qiagen). Quantitative real-time RT-PCR was performed as described previously (21) using primers shown in supplementary Table 1, available in an online appendix at <http://diabetes.diabetesjournals.org/cgi/content/full/db09-0878/DC1>. Each sample was measured in triplicates. Expression of the TATA-box binding protein (*Tbp*) and hypoxanthine guanine phosphoribosyl transferase (*Hprt*) genes were used for normalization.

Hyperinsulinemic-euglycemic clamp. Euglycemic clamps were performed in conscious 1-month-old mice using a 10 mU/kg/min insulin dose as described (22).

Insulin signaling in primary hepatocytes. Hepatocytes were isolated by a two-step perfusion protocol that is based on minor modifications of the method described by Seglen (23). Briefly, mice were anesthetized by intraperitoneal injection of pentobarbital (50 mg/kg). The abdominal cavity was opened and the liver perfused via the portal vein first with a Ca²⁺ Mg⁺⁺ free EDTA chelating solution, followed by perfusion with a Ca²⁺ Mg⁺⁺ replete buffer containing type I collagenase (Worthington Biochemical, Lakewood, NJ). The hepatocytes were then dissociated by cutting the liver capsule and gently shaking in the collagenase solution. A series of five low-speed (50g) centrifugations were performed to wash and differentially sediment hepatocytes from other cell types, particularly Kupffer and endothelial cells. The resulting cell pellet was re-suspended, and an aliquot was taken to determine cell number and viability by trypan blue exclusion. The cells were plated at a density of 2.0 \times 10⁶ cells on 60-mm collagen-coated plates (BD Biosciences, San Jose, CA) in hepto-stim media (BD Biosciences, San Jose, CA) containing 10% FBS (ATCC, Manassas, VA) and supplemented with pen/strep (ATCC,

Manassas, VA) and fungizone (Invitrogen, Carlsbad, CA) and allowed to adhere for 4 h. The media were then removed, the cells washed once with PBS, and fresh media added. The following day, the media were changed and replaced with the same media except without the fungizone. After 24 h in culture, cells were serum-starved overnight in 199 medium supplemented with glutamine, NaHCO₃, and pen/strep. After incubation in fresh serum-free media for 2 h, cells were stimulated with 100 nmol/l of porcine insulin for 10 min in triplicate wells. Cells were solubilized in lysis buffer (50 mmol/l Tris-HCl, pH 7.5, 150 mmol/l NaCl, 1% NP-40) containing inhibitors of proteases (Complete Mini; Roche, Indianapolis, IN) and phosphatases (PhosStop; Roche). Protein concentration was determined by the BCA assay (Pierce, Rockford, IL).

Immunoblot analysis. Tissue and cell lysates were analyzed with Western blotting. Primary antibodies against insulin receptor substrate (IRS)-1 (1:500 dilution, Upstate Biotechnology, Lake Placid, NY), IRS-2 (1:2,000 dilution, Upstate), Akt (1:5,000 dilution, Cell Signaling Technologies, Danvers, MA), and phospho-Akt (1:1,000 dilution, CST) were used followed by goat anti-rabbit-horseradish peroxidase (1:10,000 dilution; Jackson ImmunoResearch, West Grove, PA) secondary antibody. Blots were visualized using the ECL+ chemiluminescent detection system (Roche).

Lipase assays. The activity of lipoprotein lipase (LPL) and hepatic lipase was measured using the respective triolein substrates prepared by sonication (24). To discriminate between LPL and hepatic lipase activities further, we took advantage of the difference in salt sensitivity between these lipases. Lipase activities were measured using the LPL substrate in the presence and absence of 1 mol/l NaCl; LPL activity was calculated as the salt-inhibited fraction. Tissues were homogenized in 25 mmol/l Tris-HCl, pH 7.5, containing 10% glycerol, 0.2% deoxycholic acid (sodium salt), and 10 μ g/ml heparin. Homogenization (100 mg/ml) was carried out for 30 s on ice, using a Tekmar tissue homogenizer, followed by centrifugation for 10 min at 10,000g to remove insoluble debris and, in the case of adipose tissue, to separate the floating lipid layer from the lysate.

Statistical analysis. Data are presented as mean \pm SE. Differences between two groups were considered statistically significant at $P < 0.05$ using Student's *t* test. ANOVA was used for multiple group comparisons followed by Bonferroni's post hoc test, as implemented in the SigmaPlot software package (Systat Software, San Jose, CA). Non-normally distributed trait values were transformed before analysis as indicated.

RESULTS

Metabolic differences between young BKS-*db* and B6-*db* mice. To characterize the development of diabetes in the BKS-*db* strain, we performed a metabolic time-course study (Fig. 1, *line graphs*, and supplementary Table 3). B6-*db* mice were used as controls, because they are diabetes resistant despite their genetic similarity to BKS-*db*. Consistent with previous reports (2,4), BKS-*db* and B6-*db* mice exhibited similar body weights and adiposity, with the exception of male BKS-*db*, which started losing weight at 3 months because of severe diabetes (Fig. 1A and B). Despite similar degrees of obesity, BKS-*db* and B6-*db* mice displayed dramatic differences in glucose homeostasis. B6-*db* mice compensated for insulin resistance associated with obesity by sharply increasing plasma insulin levels (Fig. 1D). In contrast, insulin levels in BKS-*db* gradually declined and were associated with progressive hyperglycemia (Fig. 1C). These data are consistent with previous studies implicating impaired β -cell viability in BKS-*db* as the primary determinant of diabetes susceptibility (10,11,13). However, our time-course study also revealed metabolic differences between the strains at 1 month of age, before the onset of diabetes in BKS-*db* (Fig. 1, *right panels*). At this age, BKS-*db* mice maintained similar glucose levels, but over twofold higher insulin concentrations in comparison to B6-*db* mice (Fig. 1C and D). Moreover, these mice exhibited elevated plasma TG (Fig. 1E), but lower free fatty acid (Fig. 1F) and total and HDL cholesterol levels (data not shown) relative to their B6-*db* counterparts. To assess the effects of strain background and genetic interaction with the *db* mutation, we also phenotyped lean B6 and BKS mice (supplementary Table 2). Among the traits analyzed, only HDL cholesterol

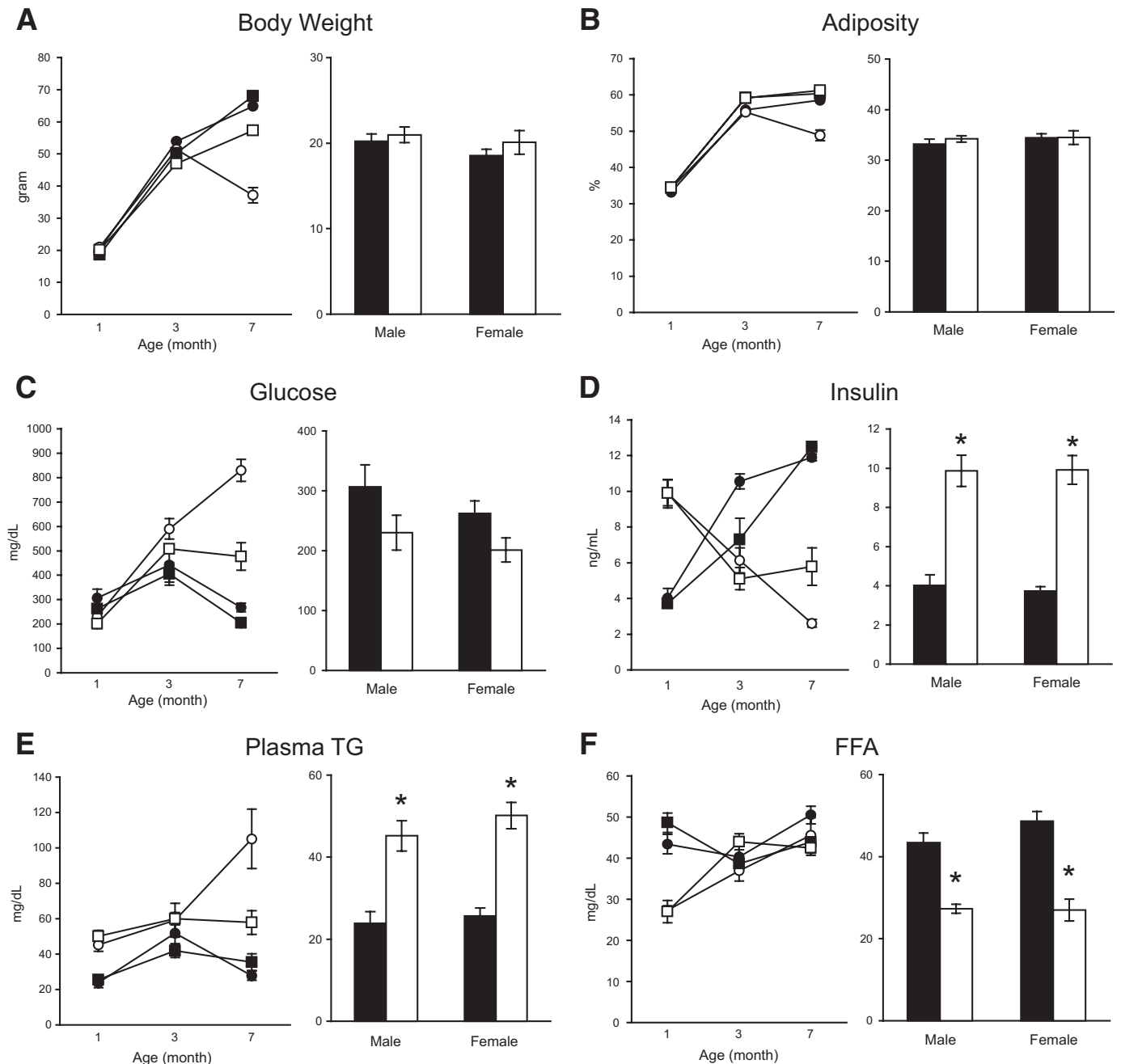


FIG. 1. Phenotype of B6-*db* and BKS-*db* mice. Body weight (A), adiposity (B), blood glucose (C), plasma insulin (D), TG (E), and free fatty acids (FFA) (F) are shown at 1, 3, and 7 months of age (left panels). ●, B6-*db* males ($n = 10$); ■, B6-*db* females ($n = 11$); ○, BKS-*db* males ($n = 10$); □, BKS-*db* females ($n = 7$). Labels of statistical significance have been omitted from the charts for clarity. Bar graphs (right panels) show data at 1 month of age. * $P < 0.05$ for differences between strains.

and insulin levels were different between wild-type B6 and BKS mice, whereas total cholesterol, free fatty acid, and glucose traits revealed significant strain \times *db* interactions. In conclusion, our results indicate β -cell-independent metabolic derangements in BKS-*db* mice. To investigate the role of different tissues in the early metabolic differences observed between B6-*db* and BKS-*db*, we further characterized 1-month-old mice in subsequent studies.

Relative muscle insulin sensitivity in young BKS-*db* mice. Differences in plasma insulin and lipid levels are frequently associated with different insulin response in different tissues. To directly investigate insulin sensitivity in young BKS-*db* and B6-*db* mice, hyperinsulinemic-eugly-

cemic clamps were performed. Upon infusion with 2.5 mU/kg/min insulin, the two strains exhibited similar metabolic parameters (data not shown). However, administration of increased doses of insulin (10 mU/kg/min) unexpectedly revealed elevated glucose infusion rate and insulin-stimulated whole-body glucose turnover in BKS-*db*, indicating better systemic insulin sensitivity in this strain (Table 1). Consistent with these results, insulin-stimulated glucose uptake in gastrocnemius muscle was also higher in BKS-*db* mice, suggesting that muscle tissue is likely responsible for their relative insulin sensitivity. In contrast, the clamp showed severe hepatic insulin resistance in both strains. In fact, even high-dose insulin infusion

TABLE 1
Hyperinsulinemic-euglycemic clamp measurements

	B6- <i>db</i>	BKS- <i>db</i>
<i>n</i>	8	6
Body weight (g)	22.1 ± 0.5	22.5 ± 0.7
Fat mass (g)	8.0 ± 0.4	7.9 ± 0.5
Lean mass (g)	12.6 ± 0.4	12.5 ± 0.5
Basal glucose (mg/dl)	125 ± 10	116 ± 19
Basal insulin (pmol/l)	328 ± 63	324 ± 53
Clamp glucose (mg/dl)	125 ± 7	135 ± 9
Clamp insulin (pmol/l)	1,882 ± 136	1,829 ± 258
Glucose infusion rate (mg/kg/min)	7.2 ± 0.9	21.3 ± 2.8*
Whole-body glucose turnover (mg/kg/min)	30.8 ± 1.4	40.6 ± 3.2†
Whole-body glycolysis (mg/kg/min)	24.2 ± 2.1	28.9 ± 1.0
Whole-body glycogen synthesis (mg/kg/min)	6.6 ± 2.0	11.7 ± 3.3
Muscle glucose uptake (nmol/g/min)	162 ± 20	314 ± 46†
Suppression of hepatic glucose production (%)	0	0

Data are means ± SE. * $P < 0.0005$; † $P < 0.05$.

failed to achieve any suppression of hepatic glucose production in either strain. In conclusion, these data indicate relative muscle insulin sensitivity in BKS-*db*, but severe hepatic insulin resistance in both strains.

Reduced insulin signaling in BKS-*db* hepatocytes. As insulin sensitivity in muscle is expected to protect against, rather than contribute to, the diabetic phenotype of BKS-*db*, we focused on liver metabolism in subsequent experiments. To investigate hepatic insulin resistance, we compared insulin signaling in the two strains. Immunoblot analysis revealed lower levels of both IRS-1 and IRS-2 proteins in BKS-*db* liver, suggesting reduced proximal insulin signaling in this strain (Fig. 2A). To confirm this prediction, we assessed downstream signaling in primary hepatocytes treated with insulin. Consistent with reduced IRS expression, insulin-stimulated Akt phosphorylation was reduced by ~50% in BKS-*db* hepatocytes (Fig. 2B). These results indicate a higher degree of hepatic insulin resistance in BKS-*db* mice.

Altered hepatic metabolism in young BKS-*db* mice. Next, we investigated the metabolic consequences of elevated hepatic insulin resistance in BKS-*db*. Upon visual examination of internal organs, BKS-*db* livers appeared darker than their B6-*db* counterparts (Fig. 3A), suggesting reduced steatosis in the former. Indeed, despite higher plasma insulin levels in BKS-*db* mice, hepatic TG content was over threefold lower in this strain (Fig. 3B). Similarly, hepatic glycogen content was also significantly reduced in BKS-*db* mice (Fig. 3E).

Because plasma free fatty acid levels are lower in BKS-*db* mice, reduced hepatic TG content may reflect reduced substrate delivery for TG biosynthesis. Alternatively, metabolic differences intrinsic to liver may also contribute to reduced steatosis in BKS-*db* mice. To discriminate between these possibilities, we used short-term in vitro liver slice cultures, which allow examination of metabolic pathways under conditions of controlled substrate delivery (15). We first examined hepatic lipogenesis by measuring the incorporation of radioactivity into de novo synthesized FAs from $^3\text{H}_2\text{O}$. Despite elevated plasma

insulin levels in vivo, the rate of hepatic lipogenesis was significantly lower in BKS-*db* liver slices (Fig. 3C), suggesting intrinsic metabolic differences in hepatic lipid synthesis between the strains. Hepatic FA oxidation was not significantly different between the two strains, although there was a trend toward increased oxidation in BKS-*db* (Fig. 3D). We also tested the potential involvement of circulating factors in the observed metabolic differences by measuring plasma levels of various adipokines and hormones implicated in hepatic metabolism (25). Plasma concentrations of adiponectin, leptin, resistin, corticosterone, and glucagon were similar in B6-*db* and BKS-*db* mice (supplementary Table 3). Taken together, our results indicate altered lipid and carbohydrate metabolism consistent with elevated hepatic insulin resistance in BKS-*db* mice.

Altered hepatic gene expression in young BKS-*db* mice. To determine if altered gene expression underlies the metabolic differences observed between BKS-*db* and B6-*db* mice, we measured mRNA levels of genes involved in hepatic lipid and carbohydrate metabolism. Consistent with reduced lipogenesis in BKS-*db* mice, expression levels of all lipogenic genes tested (liver X receptor- α [*LXR α*], sterol regulatory element binding protein-1c [*Srebp1c*], peroxisome proliferator-activated receptor- γ [*Ppar γ*], acetyl-CoA carboxylase-1 [*Acc1*], fatty acid synthase [*Fas*], ATP citrate lyase [*Acl*], stearoyl-CoA desaturase-1 [*Scd1*], and cytosolic malic enzyme [*Me1*]) were significantly lower in this strain (Fig. 4A). The expression of enzymes involved in TG synthesis, including glycerol-3-phosphate acyltransferase (*Gpat*) and lipin (*Lpin1*), was also lower in BKS-*db*. As *Srebp1c* is a direct transcriptional activator of lipogenic genes and *Gpat* (26), suppressed *Srebp1c* expression is likely to be responsible for diminished hepatic lipid synthesis in BKS-*db* mice. Other targets of *Srebp1c*, such as glucokinase (*Gk*) and the FA transporter *Cd36*, also exhibited reduced expression in this strain. In contrast, mRNA levels of acyl-CoA:diacylglycerol acyltransferase-2 (*Dgat2*), a TG biosynthetic enzyme not known to be regulated by *Srebp1c*, were similar in the two strains.

We also analyzed gluconeogenic gene expression (Fig. 4B). After a 4-h fast, which results in more than twofold higher insulin levels in BKS-*db* than in B6-*db* mice (Fig. 4B, left panel), the mRNA levels of phosphoenopyruvate carboxykinase (*Pepck*), fructose-1,6-bisphosphatase (*Fbp*), and glucose-6-phosphatase (*G6p*) were similar in the two strains (Fig. 4B, right panel). Conversely, similar plasma insulin levels after an overnight fast were associated with elevated expression of *Pepck* and *Fbp*, but not *G6p*, in BKS-*db* mice (Fig. 4B). In conclusion, our gene expression results indicate diminished hepatic insulin action in BKS-*db* mice. Consistent with a proximal defect in insulin signaling, hepatic insulin resistance affects both the lipogenic and anti-gluconeogenic actions of insulin in this strain.

Reduced TG clearance in young BKS-*db* mice. BKS-*db* mice exhibit twofold higher plasma TG levels than B6-*db* mice at 1 month of age (Fig. 1E, right panel). Considering the lower hepatic TG content in BKS-*db* mice (Fig. 3B), this result was initially surprising. To investigate the mechanisms underlying these differences, we measured hepatic TG secretion in 1-month-old mice after inhibiting clearance with Triton WR1339. This analysis indicated similar rates of hepatic TG secretion in B6-*db* and BKS-*db* mice (Fig. 5A). As plasma TG levels are determined by the relative rates of secretion and clearance, we also mea-

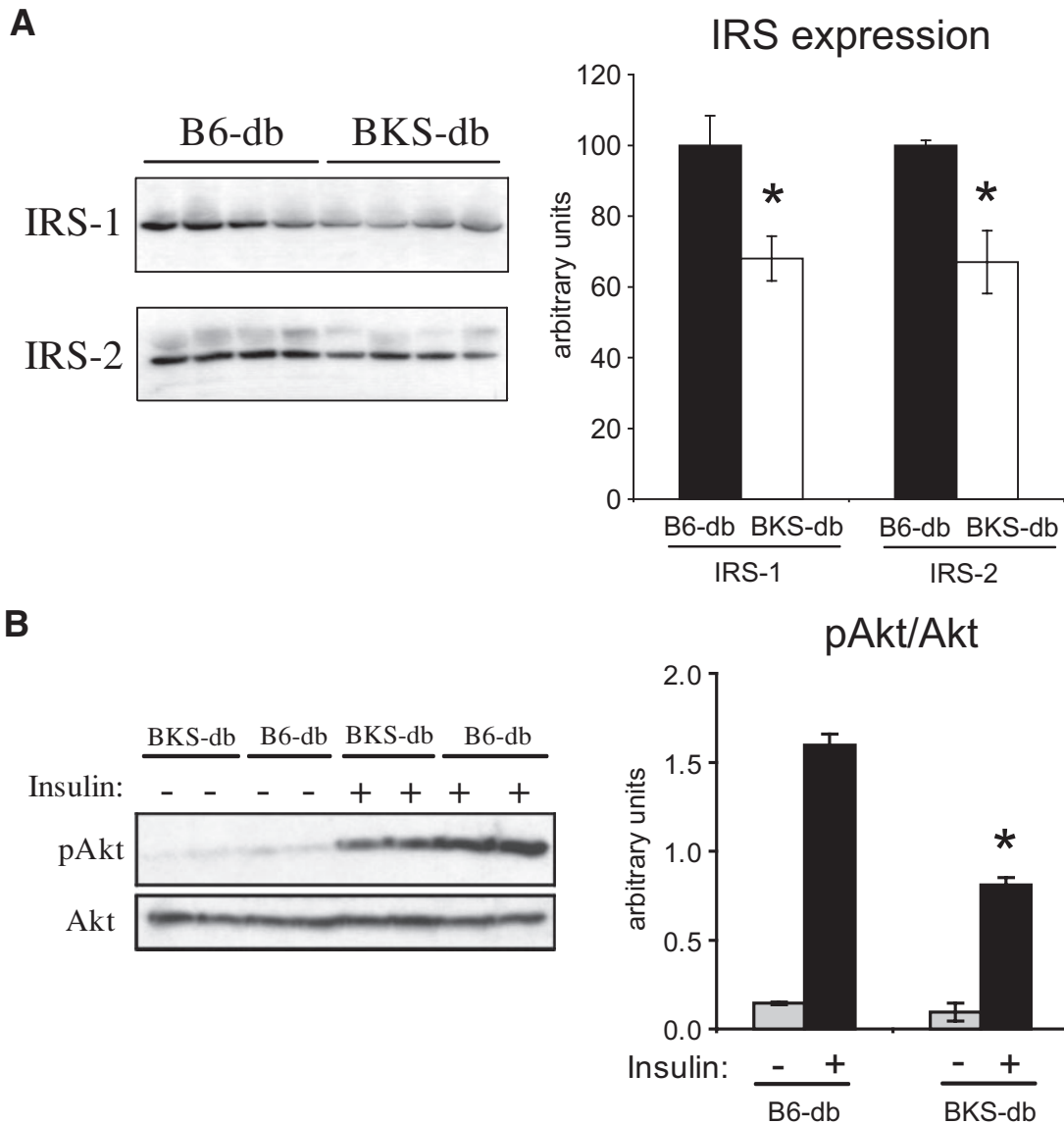


FIG. 2. A: Western blots showing hepatic IRS-1 and IRS-2 expression in B6-*db* and BKS-*db* mice. Each lane represents equal total protein loading from individual animals. **B:** Insulin signaling in primary hepatocytes. Hepatocyte cultures were stimulated with 100 nmol/l insulin for 10 min. Western blots show phosphorylated Akt (*upper panel*) and total Akt (*lower panel*). Graphs on the right represent densitometric analysis of band intensities. * $P < 0.05$.

sured plasma TG clearance after an oral lipid load. In B6-*db* mice, lipid ingestion resulted in a modest (less than twofold) rise in plasma TG levels peaking at 2 h after gavage and returning to baseline levels after 4 h (Fig. 5B). In contrast, BKS-*db* mice exhibited an over fourfold increase in TG at 2 h, and TG levels remained elevated threefold after 4 h. These data indicate significantly reduced clearance of circulating TG in BKS-*db* mice.

To test the potential role of lipases in reduced TG clearance in BKS-*db* mice, we measured the activities of these enzymes in postheparin plasma. Consistent with reduced TG clearance, total lipase, LPL, and hepatic lipase activities are significantly lower in BKS-*db* plasma (Fig. 5C). To identify the tissue(s) responsible for differences in LPL activity, we assayed lipase activity in isolated tissues (Fig. 5D). Adipose and, to a smaller extent, heart from BKS-*db* mice exhibit lower LPL activities, whereas skeletal muscle shows the opposite pattern. In conclusion, these data suggest that elevated plasma TG levels in BKS-*db*

mice result from reduced clearance primarily due to low LPL activity in adipose. Further studies will be required to explore the underlying mechanisms in this tissue.

DISCUSSION

Mutations in the leptin receptor gene cause severe obesity and insulin resistance in rodents and humans (27–29). In leptin receptor-deficient (*db* mutation) mouse strains, obesity is variably associated with hyperglycemia depending on genetic background (30). Diabetes-resistant strains, such as B6-*db*, exhibit islet hypertrophy and insulin hypersecretion and are able to maintain mildly elevated plasma glucose levels. In contrast, islets in the diabetes-susceptible BKS-*db* strain undergo atrophy leading to insulin deficiency and hyperglycemia. The genes underlying these phenotypic differences are largely unknown. Based on reduced viability and proliferative capacity of BKS β -cells both in vivo and in vitro, diabetes susceptibility of this

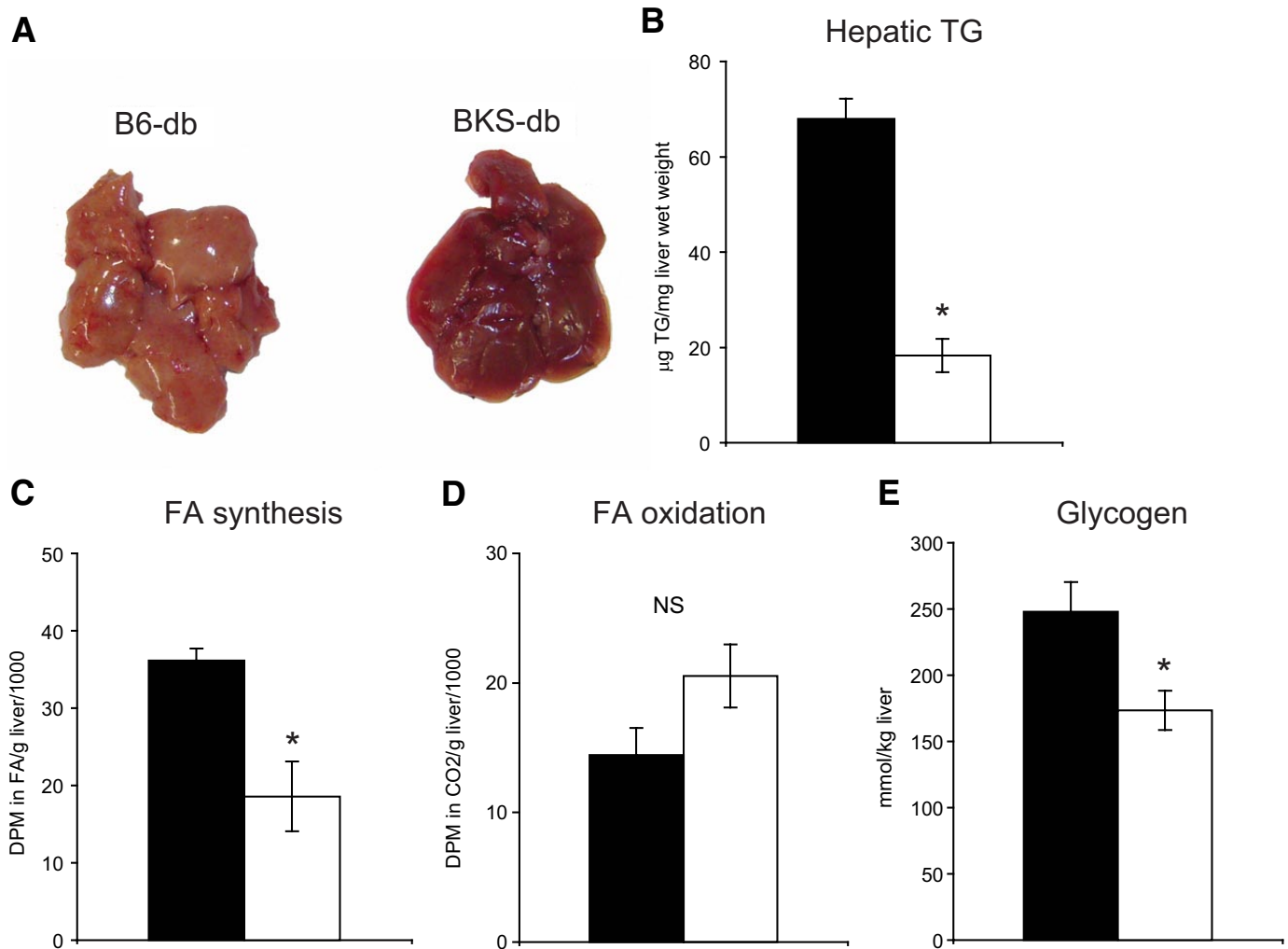


FIG. 3. Hepatic fatty acid metabolism in 1-month-old male B6-*db* (■) and BKS-*db* (□) mice. **A:** Representative images of B6-*db* and BKS-*db* livers. **B:** Hepatic TG content in B6-*db* ($n = 10$) and BKS-*db* ($n = 10$) mice. Rates of *in vitro* FA synthesis (**C**) ($n = 4 + 4$) and oxidation ($n = 7 + 7$) in liver slice cultures (**D**) are shown. **E:** Hepatic glycogen content ($n = 10 + 10$). DPM, disintegration per minute. * $P < 0.05$. (A high-quality color representation of this figure is available in the online issue.)

strain has been ascribed to genetic determinants acting in islets (10–13). However, it is conceivable that genetic differences manifested in other tissues may also contribute to β -cell failure through mechanisms that increase metabolic stress on these cells (e.g., insulin resistance). Indeed, in the current study, we demonstrate increased hepatic insulin resistance in young BKS-*db* mice compared with B6-*db* mice and propose that this metabolic abnormality may lead to elevated β -cell stress and the diabetic phenotype in BKS-*db*.

Side-by-side phenotypic characterization of BKS-*db* and B6-*db* mice revealed differences in plasma lipid and insulin levels as early as 1 month of age, even before the onset of β -cell dysfunction in BKS-*db* mice. These observations indicated metabolic differences in tissues other than β -cells and prompted us to investigate the early BKS-*db* phenotype further. Unexpectedly, hyperinsulinemic-euglycemic clamp studies demonstrated higher whole-body and muscle insulin sensitivity in BKS-*db*, indicating that this tissue does not contribute to, but rather counteracts, the diabetes-sensitive phenotype of this strain. However, the clamp also revealed profound hepatic insulin resistance, which completely abolished the effect of high doses of insulin on hepatic glucose production in both strains.

However, in contrast to muscle, hepatic insulin resistance is more severe in BKS-*db* than B6-*db* mice. Despite elevated plasma insulin levels, BKS-*db* mice exhibit signs of reduced hepatic insulin action including diminished lipogenesis, glycogen accumulation, insulin-stimulated gene expression and TG secretion, and suppression of gluconeogenic gene expression. Furthermore, direct analysis of hepatic insulin signaling demonstrated lower IRS-1 and IRS-2 expression as well as insulin-stimulated Akt phosphorylation in BKS-*db* hepatocytes. Diminished IRS-1/2 expression has been linked to reduced hepatic insulin signaling in various obese animal models in comparison to their lean counterparts (31–34). Thus, our data suggest that lower IRS-1/2 expression in BKS-*db* mice results in relative hepatic insulin resistance in this strain.

Hepatic insulin resistance is a principal component of type 2 diabetes (35). Decreased insulin sensitivity in liver leads to elevated hepatic glucose production, hyperinsulinemia, increased β -cell stress, and hyperglycemia (36). Animal models indicate that hepatic insulin resistance can play a primary role in the development of diabetes (37). For example, diminished insulin signaling due to hepatic insulin receptor (38) or IRS-1/2 deficiency (34,39) causes hyperglycemia. In line with these studies, we propose that

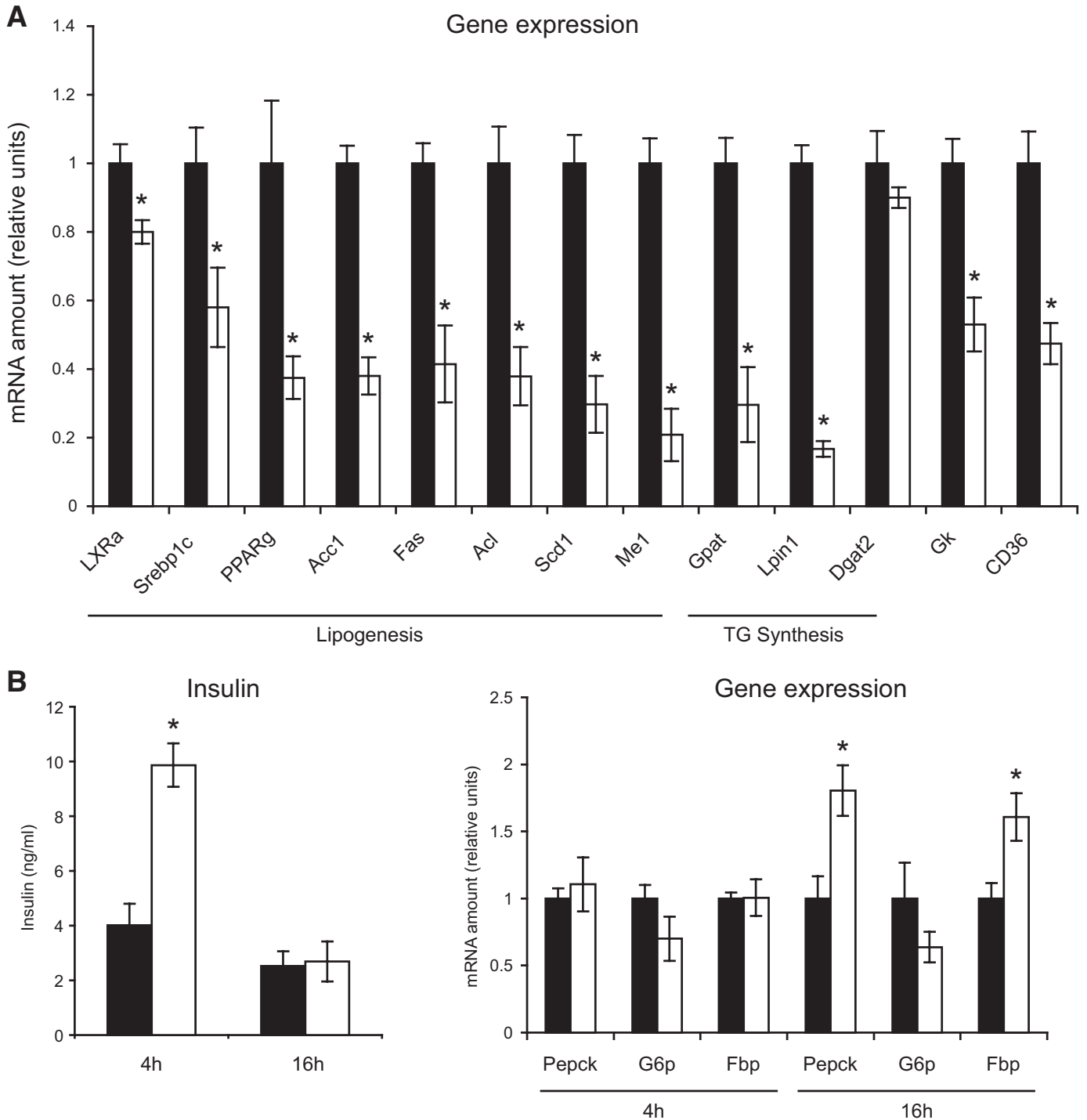


FIG. 4. A: Hepatic mRNA levels for enzymes involved in lipogenesis and TG synthesis in 1-month-old male B6-*db* (■, *n* = 5) and BKS-*db* (□, *n* = 5) mice fasted for 4 h. Relative mRNA levels are normalized to B6-*db* values. **B: Left panel:** Plasma insulin levels after 4 h (*n* = 10 + 10) and 16 h (*n* = 5–5) of fasting. **Right panel:** Gluconeogenic gene expression after 4 h (*n* = 5 + 5) and 16 h of fasting (*n* = 5 + 5). **P* < 0.05 for differences between strains.

early hepatic insulin resistance in BKS-*db* mice contributes to the diabetes-susceptible phenotype of this strain.

What are the metabolic consequences of hepatic insulin resistance in BKS-*db* mice? Although we did not directly demonstrate it in our study, hepatic glucose output is expected to be higher in BKS-*db* mice than in B6-*db* mice. Diminished insulin signaling in BKS-*db* liver results in impaired suppression of gluconeogenic gene expression and likely elevated glycogenolysis, consistent with lower

hepatic glycogen content observed in this strain. Another relevant finding is markedly reduced lipogenic capacity in the BKS-*db* liver. It has been proposed that active lipogenesis reduces fuel partitioning into the gluconeogenic pathway, thereby reducing the rate of glucose production at the substrate level (40). Thus, reduced lipogenesis resulting from proximal defects in insulin signaling in BKS-*db* mice may contribute to elevated gluconeogenesis, increased β-cell stress, and the development of diabetes in

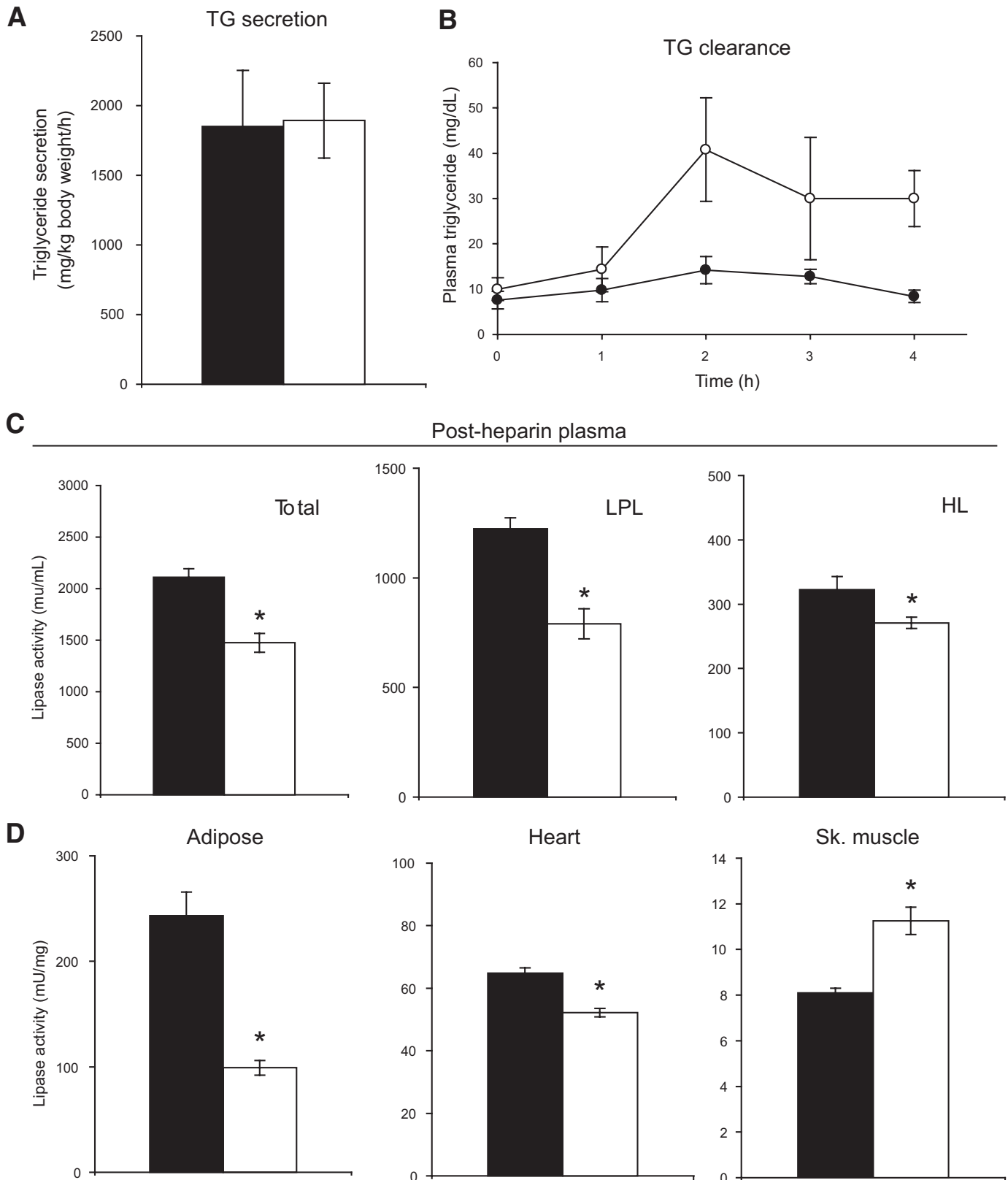


FIG. 5. **A:** Hepatic TG secretion in 1-month-old male B6-*db* (■, $n = 4$) and BKS-*db* (□, $n = 6$) mice as measured after the intravenous injection of Triton. **B:** TG clearance after an oral lipid load ($n = 5-5$). **C:** Postheparin plasma levels of total lipase activity, LPL, and hepatic lipase (HL). **D:** Lipase activities in adipose, heart, and skeletal (Sk.) muscle tissues. A total of 4–6 animals of each strain were averaged in lipase activity measurements. * $P > 0.05$ for differences between strains.

this strain. Consistent with this hypothesis, decreased hepatic lipogenesis and steatosis are also associated with diabetes susceptibility in the obese BTBR-*ob* (40), lipatro-

phic FVB-AZIP (41), and liver-specific Ppary knockout mouse models (42). Moreover, increased hepatic lipogenesis and steatosis achieved by overexpressing Srebp1c

(43) or the administration of Ppar γ (44,45) or LXR agonists (46) markedly improve glycemia in diabetic mice.

In addition to β -cells and liver, metabolic abnormalities in other tissues may also contribute to the development of diabetes in BKS-*db* mice. For example, our results suggest that low LPL activity in BKS-*db* adipose tissue is associated with reduced clearance and elevated levels of plasma TG, which may inflict lipotoxic stress in β -cells (47). Further studies will be needed to address the potential contribution of adipose tissue to the diabetic phenotype.

ACKNOWLEDGMENTS

This work was supported by National Institutes of Health Grants DK071673 and DK80756, the Cedars-Sinai Medical Center, and American Diabetes Association Grants 1-05-RA-96 and 7-07-RA-80.

No potential conflicts of interest relevant to this article were reported.

The authors thank Dr. Nicole Ehrhardt for expert statistical analysis.

REFERENCES

- Hummel KP, Dickie MM, Coleman DL. Diabetes, a new mutation in the mouse. *Science* 1966;153:1127–1128
- Hummel KP, Coleman DL, Lane PW. The influence of genetic background on expression of mutations at the diabetes locus in the mouse. I. C57BL-KsJ and C57BL-6J strains. *Biochem Genet* 1972;7:1–13
- Coleman DL, Hummel KP. The influence of genetic background on the expression of the obese (Ob) gene in the mouse. *Diabetologia* 1973;9:287–293
- Coleman DL, Hummel KP. Symposium IV: Diabetic syndrome in animals. Influence of genetic background on the expression of mutations at the diabetes locus in the mouse. II. Studies on background modifiers. *Isr J Med Sci* 1975;11:708–713
- Kaku K, Province M, Permutt MA. Genetic analysis of obesity-induced diabetes associated with a limited capacity to synthesize insulin in C57BL/KS mice: evidence for polygenic control. *Diabetologia* 1989;32:636–643
- Naggert JK, Mu JL, Frankel W, Bailey DW, Paigen B. Genomic analysis of the C57BL/Ks mouse strain. *Mamm Genome* 1995;6:131–133
- Mao HZ, Roussos ET, Péterfy M. Genetic analysis of the diabetes-prone C57BLKS/J mouse strain reveals genetic contribution from multiple strains. *Biochim Biophys Acta* 2006;1762:440–446
- Davis RC, Schadt EE, Cervino AC, Péterfy M, Lusis AJ. Ultrafine mapping of SNPs from mouse strains C57BL/6J, DBA/2J, and C57BLKS/J for loci contributing to diabetes and atherosclerosis susceptibility. *Diabetes* 2005;54:1191–1199
- Like AA, Chick WL. Studies in the diabetic mutant mouse. I. Light microscopy and radioautography of pancreatic islets. *Diabetologia* 1970;6:207–215
- Cohn JA, Cerami A. The influence of genetic background on the susceptibility of mice to diabetes induced by alloxan and on recovery from alloxan diabetes. *Diabetologia* 1979;17:187–191
- Rossini AA, Appel MC, Williams RM, Like AA. Genetic influence of the streptozotocin-induced insulinitis and hyperglycemia. *Diabetes* 1977;26:916–920
- Leiter EH. Multiple low-dose streptozotocin-induced hyperglycemia and insulinitis in C57BL mice: influence of inbred background, sex, and thymus. *Proc Natl Acad Sci U S A* 1982;79:630–634
- Swenne I, Andersson A. Effect of genetic background on the capacity for islet cell replication in mice. *Diabetologia* 1984;27:464–467
- Mehrabian M, Qiao JH, Hyman R, Ruddle D, Laughton C, Lusis AJ. Influence of the apoA-II gene locus on HDL levels and fatty streak development in mice. *Arterioscler Thromb* 1993;13:1–10
- Olinga P, Groen K, Hof IH, De Kanter R, Koster HJ, Leeman WR, Rutten AA, Van Twillert K, Groothuis GM. Comparison of five incubation systems for rat liver slices using functional and viability parameters. *J Pharmacol Toxicol Methods* 1997;38:59–69
- Olubadewo J, Morgan DW, Heimberg M. Effects of triiodothyronine on biosynthesis and secretion of triglyceride by livers perfused in vitro with [3H]oleate and [14C]glycerol. *J Biol Chem* 1983;258:938–945
- Lowenstein JM, Brunengraber H, Wadke M. Measurement of rates of lipogenesis with deuterated and tritiated water. *Methods Enzymol* 1975;35:279–287
- Castellani LW, Wilcox HC, Heimberg M. Relationships between fatty acid synthesis and lipid secretion in the isolated perfused rat liver: effects of hyperthyroidism, glucose and oleate. *Biochim Biophys Acta* 1991;1086:197–208
- Tietge UJ, Bakillah A, Maugeais C, Tsukamoto K, Hussain M, Rader DJ. Hepatic overexpression of microsomal triglyceride transfer protein (MTP) results in increased in vivo secretion of VLDL triglycerides and apolipoprotein B. *J Lipid Res* 1999;40:2134–2139
- Weinstein MM, Yin L, Beigneux AP, Davies BS, Gin P, Estrada K, Melford K, Bishop JR, Esko JD, Dallinga-Thie GM, Fong LG, Bensadoun A, Young SG. Abnormal patterns of lipoprotein lipase release into the plasma in GPIIBP1-deficient mice. *J Biol Chem* 2008;283:34511–34518
- Phan J, Péterfy M, Reue K. Lipin expression preceding peroxisome proliferator-activated receptor- γ is critical for adipogenesis in vivo and in vitro. *J Biol Chem* 2004;279:29558–29564
- Kim HJ, Higashimori T, Park SY, Choi H, Dong J, Kim YJ, Noh HL, Cho YR, Cline G, Kim YB, Kim JK. Differential effects of interleukin-6 and -10 on skeletal muscle and liver insulin action in vivo. *Diabetes* 2004;53:1060–1067
- Seglen PO. Preparation of isolated rat liver cells. *Methods Cell Biol* 1976;13:29–83
- Briquet-Laugier V, Ben-Zeev O, Doolittle MH. Determining lipoprotein lipase and hepatic lipase activity using radiolabeled substrates. *Methods Mol Biol* 1999;109:81–94
- Guerre-Millo M. Adipose tissue and adipokines: for better or worse. *Diabete Metab* 2004;30:13–19
- McPherson R, Gauthier A. Molecular regulation of SREBP function: the Insig-SCAP connection and isoform-specific modulation of lipid synthesis. *Biochem Cell Biol* 2004;82:201–211
- Chen H, Charlat O, Tartaglia LA, Woolf EA, Weng X, Ellis SJ, Lakey ND, Culpepper J, Moore KJ, Breitbart RE, Duyk GM, Tepper RI, Morgenstern JP. Evidence that the diabetes gene encodes the leptin receptor: identification of a mutation in the leptin receptor gene in db/db mice. *Cell* 1996;84:491–495
- Chua SC Jr, Chung WK, Wu-Peng XS, Zhang Y, Liu SM, Tartaglia L, Leibel RL. Phenotypes of mouse diabetes and rat fatty due to mutations in the OB (leptin) receptor. *Science* 1996;271:994–996
- Clément K, Vaisse C, Lahlou N, Cabrol S, Pelloux V, Cassuto D, Gormelen M, Dina C, Chambaz J, Lacorte JM, Basdevant A, Bougnères P, Lebouc Y, Froguel P, Guy-Grand B. A mutation in the human leptin receptor gene causes obesity and pituitary dysfunction. *Nature* 1998;392:398–401
- Clee SM, Attie AD. The genetic landscape of type 2 diabetes in mice. *Endocr Rev* 2007;28:48–83
- Anai M, Funaki M, Ogihara T, Terasaki J, Inukai K, Katagiri H, Fukushima Y, Yazaki Y, Kikuchi M, Oka Y, Asano T. Altered expression levels and impaired steps in the pathway to phosphatidylinositol 3-kinase activation via insulin receptor substrates 1 and 2 in Zucker fatty rats. *Diabetes* 1998;47:13–23
- Saad MJ, Araki E, Miralpeix M, Rothenberg PL, White MF, Kahn CR. Regulation of insulin receptor substrate-1 in liver and muscle of animal models of insulin resistance. *J Clin Invest* 1992;90:1839–1849
- Kerouz NJ, Hörsch D, Pons S, Kahn CR. Differential regulation of insulin receptor substrates-1 and -2 (IRS-1 and IRS-2) and phosphatidylinositol 3-kinase isoforms in liver and muscle of the obese diabetic (ob/ob) mouse. *J Clin Invest* 1997;100:3164–3172
- Suzuki R, Tobe K, Aoyama M, Inoue A, Sakamoto K, Yamauchi T, Kamon J, Kubota N, Terauchi Y, Yoshimatsu H, Matsuhisa M, Nagasaka S, Ogata H, Tokuyama K, Nagai R, Kadowaki T. Both insulin signaling defects in the liver and obesity contribute to insulin resistance and cause diabetes in Irs2(-/-) mice. *J Biol Chem* 2004;279:25039–25049
- DeFronzo RA. Pathogenesis of type 2 diabetes: metabolic and molecular implications for identifying diabetes genes. *Diabetes Rev* 1997;5:177–269
- Biddinger SB, Kahn CR. From mice to men: insights into the insulin resistance syndromes. *Annu Rev Physiol* 2006;68:123–158
- Haas JT, Biddinger SB. Dissecting the role of insulin resistance in the metabolic syndrome. *Curr Opin Lipidol* 2009;20:206–210
- Michael MD, Kulkarni RN, Postic C, Previs SF, Shulman GI, Magnuson MA, Kahn CR. Loss of insulin signaling in hepatocytes leads to severe insulin resistance and progressive hepatic dysfunction. *Mol Cell* 2000;6:87–97
- Taniguchi CM, Ueki K, Kahn R. Complementary roles of IRS-1 and IRS-2 in the hepatic regulation of metabolism. *J Clin Invest* 2005;115:718–727
- Lan H, Rabaglia ME, Stoehr JP, Nadler ST, Schueler KL, Zou F, Yandell BS, Attie AD. Gene expression profiles of nondiabetic and diabetic obese mice suggest a role of hepatic lipogenic capacity in diabetes susceptibility. *Diabetes* 2003;52:688–700

41. Colombo C, Haluzik M, Cutson JJ, Dietz KR, Marcus-Samuels B, Vinson C, Gavrilova O, Reitman ML. Opposite effects of background genotype on muscle and liver insulin sensitivity of lipoatrophic mice: role of triglyceride clearance. *J Biol Chem* 2003;278:3992–3999
42. Matsusue K, Haluzik M, Lambert G, Yin SH, Gavrilova O, Ward JM, Brewer B Jr, Reitman ML, Gonzalez FJ. Liver-specific disruption of PPARgamma in leptin-deficient mice improves fatty liver but aggravates diabetic phenotypes. *J Clin Invest* 2003;111:737–747
43. Bécard D, Hainault I, Azzout-Marniche D, Bertry-Cousot L, Ferré P, Foufelle F. Adenovirus-mediated overexpression of sterol regulatory element binding protein-1c mimics insulin effects on hepatic gene expression and glucose homeostasis in diabetic mice. *Diabetes* 2001;50:2425–2430
44. Suzuki A, Yasuno T, Kojo H, Hirosumi J, Mutoh S, Notsu Y. Alteration in expression profiles of a series of diabetes-related genes in db/db mice following treatment with thiazolidinediones. *Jpn J Pharmacol* 2000;84:113–123
45. Bedoucha M, Atzpodien E, Boelsterli UA. Diabetic KKAY mice exhibit increased hepatic PPARgamma1 gene expression and develop hepatic steatosis upon chronic treatment with antidiabetic thiazolidinediones. *J Hepatol* 2001;35:17–23
46. Cao G, Liang Y, Broderick CL, Oldham BA, Beyer TP, Schmidt RJ, Zhang Y, Stayrook KR, Suen C, Otto KA, Miller AR, Dai J, Foxworthy P, Gao H, Ryan TP, Jiang XC, Burris TP, Eacho PI, Etgen GJ. Antidiabetic action of a liver x receptor agonist mediated by inhibition of hepatic gluconeogenesis. *J Biol Chem* 2003;278:1131–1136
47. Unger RH. Lipotoxic diseases. *Annu Rev Med* 2002;53:319–336